

PCCP

Accepted Manuscript



This article can be cited before page numbers have been issued, to do this please use: A. Buytendyk, J. D. Graham, K. Collins, K. H. Bowen, C. Wu and J. I. Wu, *Phys. Chem. Chem. Phys.*, 2015, DOI: 10.1039/C5CP04754D.



This is an *Accepted Manuscript*, which has been through the Royal Society of Chemistry peer review process and has been accepted for publication.

Accepted Manuscripts are published online shortly after acceptance, before technical editing, formatting and proof reading. Using this free service, authors can make their results available to the community, in citable form, before we publish the edited article. We will replace this *Accepted Manuscript* with the edited and formatted *Advance Article* as soon as it is available.

You can find more information about *Accepted Manuscripts* in the [Information for Authors](#).

Please note that technical editing may introduce minor changes to the text and/or graphics, which may alter content. The journal's standard [Terms & Conditions](#) and the [Ethical guidelines](#) still apply. In no event shall the Royal Society of Chemistry be held responsible for any errors or omissions in this *Accepted Manuscript* or any consequences arising from the use of any information it contains.

The Hydrogen Bond Strength of the Phenol-Phenolate Anionic Complex: A Computational and Photoelectron Spectroscopic Study

Allyson M. Buytendyk[§], Jacob D. Graham[§], Kim D. Collins[‡] and Kit H. Bowen^{*§}

[§] Department of Chemistry, Johns Hopkins University, Baltimore, MD 21218, USA

[‡] IMET and Department of Microbiology and Immunology, University of Maryland School of Medicine, Baltimore, MD 21201, USA

Chia-Hua Wu[#] and Judy I. Wu[#]

[#] Department of Chemistry, University of Houston, Houston, TX 77204, USA

*Correspondence should be addressed to K.H.B.: e-mail: kbowen@jhu.edu, phone: (410) 516-8425 or J.I.W.: e-mail: jiwu@central.uh.edu, phone: (713) 743-7719.

Abstract

The phenol-phenolate anionic complex was studied *in vacuo* by negative ion photoelectron spectroscopy using 193 nm photons and by density functional theory (DFT) computations at the ω B97XD/6-311+G(2d,p) level. We characterize the phenol-phenolate anionic complex as a proton-coupled phenolate pair, i.e., as a low-barrier hydrogen bond system. Since the phenol-phenolate anionic complex was studied in the gas phase, its measured hydrogen bond strength is its maximal ionic hydrogen bond strength. The $D(\text{PhO}^- \cdots \text{HOPh})$ interaction energy (26-30 kcal/mol), i.e., the hydrogen bond strength in the $\text{PhO}^- \cdots \text{HOPh}$ complex, is quite substantial. Block-localized wavefunction (BLW) computations reveal that hydrogen bonded phenol rings exhibit increased ring π -electron delocalization energies compared to the free phenol monomer. This additional stabilization may explain the stronger than expected proton donating ability of phenol.

1. Introduction

Phenol and its chemical derivatives are important building blocks in biological systems. Phenol is the side-chain functional group in the amino acid, tyrosine. Deprotonated phenol, i.e., the phenolate anion, enjoys enhanced stabilization due to the delocalization of its excess charge onto the aromatic ring.¹⁻⁵ For this reason, phenol exhibits slightly higher gas-phase acidity than most alcohols.⁶⁻⁹ While the correlation between electronegativities and hydrogen bond strengths in OH/O- proton-coupled complexes has been studied theoretically,¹⁰⁻¹³ there have been no gas-phase experiments involving the phenol-phenolate anions.

The phenol-phenolate anionic complex can also be viewed as a likely example of an ionic, low-barrier hydrogen bond (LBHB). In a LBHB, a proton is shared between anions whose

conjugate acids have matching or near matching pK_a values. Some enzymologists postulate that the remarkable rate enhancements seen in enzyme catalysis are due in part to the formation of strong, short LBHBs.¹⁴⁻¹⁸ A ^1H NMR study by Mildvan and coworkers¹⁹ provided evidence for the existence of a LBHB between the phenolic proton of the Tyr-14 side chain in the enzyme active site of Δ^5 -3-ketosteroid isomerase (KSI) and the dienolate reaction intermediate. The strength of that hydrogen bond was estimated to be at least 7.1 kcal/mol (0.31 eV), whereas typical hydrogen bond strengths in proteins are somewhat smaller. In the gas phase (*in vacuo*), this value might be expected to be significantly larger, because competition among hydrogen bonding partners in condensed phase environments usually reduces hydrogen bond strengths compared to those in the gas phase, where there is no competition. We view the gas-phase, phenol-phenolate anionic complex as an elementary model for the above enzymatic interaction.

2. Methods

2.1 Experimental

Anion photoelectron spectroscopy is conducted by crossing a mass-selected beam of negative ions with a fixed-frequency photon beam and energy-analyzing the resultant photodetached electrons. Photodetachment transitions occur between the ground state of a mass-selected negative ion and the ground and energetically accessible excited states of its neutral counterpart. This process is governed by the energy-conserving relationship $h\nu = \text{EBE} + \text{EKE}$, where $h\nu$ is the photon energy, EBE is the electron binding energy, and EKE is the electron kinetic energy. Measuring electron kinetic energies and knowing the photon energy provides electron binding (photodetachment transition) energies. Because these are vertical transitions, their relative intensities are determined by the extent of Franck–Condon overlap between the anion and its corresponding neutral. Our apparatus consists of a laser photoemission anion source, a linear time-of-flight mass spectrometer for mass analysis and mass selection, a magnetic bottle electron energy analyzer, and an ArF excimer laser. The magnetic bottle has a resolution of ~ 50 meV at an EKE of 1 eV. In these experiments, photoelectron spectra were recorded with 193 nm (6.42 eV) photons. The photoelectron spectra were calibrated against the well-known transitions of atomic Cu⁻. A description of our apparatus has been reported elsewhere.²⁰

To produce the phenolate and phenol–phenolate anions, phenol was placed in a small oven (~ 25 °C) attached to the front of a pulsed (10 Hz) valve (General Valve Series 9), where helium (~ 45 psia) was expanded over the sample in a high vacuum chamber (10^{-6} Torr). Just outside the orifice of the oven, low-energy electrons were produced by laser/photoemission from a pulsed Nd:YAG laser beam (10 Hz, 532 nm) striking a translating, rotating, copper rod (6.35 mm diameter). Negatively-charged anions were then pulse-extracted into the spectrometer prior to mass selection and photodetachment.

2.2 Computational

Geometry optimizations for the phenol, phenolate, and phenol–phenolate complex (both radical and anionic forms) as well as the electron affinity of phenolate, EA(PhO), the electron

affinity of the phenol-phenolate complex, EA((PhO₂)H), the dissociation energy of the neutral phenol-phenolate complex, D(PhO \cdots HOPh), and the dissociation energy of the anionic phenol-phenolate complex dissociating into those two units, D(PhO \cdots HOPh), values were computed at ω B97XD²¹/6-311+G(2d,p)²² (all energies reported include zero-point energy corrections). Minima structures were located and vibrational frequency analyses verified the nature of the stationary points. Basis set superposition error (BSSE) corrections to the hydrogen bonding interaction energies were computed using the counterpoise approach.²³ All computations were performed in Gaussian 09.²⁴

Block-localized wavefunction (BLW)²⁵ computations quantified the π -resonance energies (RE) of the free (monomer) and hydrogen bonded phenol, following the Pauling-Wheland resonance energy definition. The BLW-RE's were computed by the total energy of the fully delocalized wavefunction (Ψ_{deloc}) of the phenol ring considered minus that of a localized wavefunction (Ψ_{loc}), in which π -conjugation among the C=C π -bonds were artificially "turned off" (BLW-RE = $\Psi_{\text{deloc}} - \Psi_{\text{loc}}$). Ψ_{loc} is computed by partitioning all of the electrons and basis functions of the molecule considered into four subspaces ("blocks"): three for each of the π -C=C units (each block includes two π -electrons, as well as the p_z , d_{xz} , and d_{yz} basis functions for each carbon atom) and one for the remainder of the molecule (including the remaining electrons and basis functions); orbitals of the same subspaces are mutually orthogonal but orbitals of different subspaces overlap freely. Both Ψ_{deloc} and Ψ_{loc} are self-consistently optimized. All vertical BLW-RE computations were performed at B3LYP/6-31G(d)// ω B97XD/6-311+G(2d,p).

3. Results and Analysis

The photoelectron spectrum of the phenolate anion, PhO $^-$ is presented in Figure 1(a). Three distinct bands are present. The $v'=0 \leftarrow v''=0$ (origin) transition resides under the lowest EBE band. Our photoelectron spectrum of the phenolate anion is in agreement with those reported previously.¹⁻⁴ In extracting the electron affinity value from our photoelectron spectrum of the PhO $^-$ anion, we benefited from previous anion photoelectron studies of PhO $^-$. Lineberger and co-workers¹ determined the EA(PhO) value to be 2.2530 ± 0.0060 eV; Fielding and co-workers² reported an EA(PhO) value of 2.15 ± 0.15 eV; Neumark and co-workers³ assigned an EA(PhO) value of 2.25380 ± 0.00080 eV; and Wang and co-workers⁴ determined EA(PhO) value to be 2.25317 ± 0.00037 eV. While our photoelectron spectrum of the PhO $^-$ anion was recorded at lower resolution, it is fully consistent with those previously recorded, allowing us to locate the EBE value of its origin transition on the spectral profile observed in this study. Our computational EA(PhO) value of 2.16 eV is also in good agreement with the previously reported experimental values, validating our theoretical methods, but also providing a measure of the accuracy of those methods.

The photoelectron spectrum of the phenol-phenolate anionic complex, PhO $^- \cdots$ HOPh, is presented in Figure 1(b). It exhibits at least two broad features, with the onset of the first transition occurring at 3.0 eV. Although an electron affinity cannot be confidently assigned to the PhO $^- \cdots$ HOPh anion spectrum, an empirical threshold value (E_T), based on a linear extrapolation of the steepest rise on the low EBE side of the lowest EBE band in the spectrum, was determined to be $3.16 \text{ eV} \pm 0.15 \text{ eV}$. Our calculated EA((PhO)₂H) value was 3.01 eV. This is consistent with

our photoelectron spectrum of the $\text{PhO}^- \cdots \text{HOPh}$ anion, and it is close to our estimated threshold value.

In our previous LBHB work²⁶ we looked to the anion photoelectron studies of six hydrogen bihalide anions, HX_2^- , where X denoted both homogeneous and heterogeneous combinations of the halogen atoms, Cl, Br, and I, as guides for interpreting our photoelectron spectra and for extracting hydrogen bond strengths, i.e., $D(\text{X}^- \cdots \text{HX})$, directly from them. The simpler hydrogen bihalide anions are in many ways analogous to more chemically complicated proton-coupled LBHB systems. Neumark and co-workers^{27,28} found the $\text{X} \cdots \text{HX}$ neutral complexes, resulting from photodetachment of HX_2^- , to be unbound. Our computations involving the phenol-phenolate system, however, found the $\text{PhO}^- \cdots \text{HOPh}$ neutral complex to be bound by 0.36 eV. Thus, the sought-after hydrogen bond strength of the PhO^-/HOPh couple cannot be estimated solely from the photoelectron spectral data.

The phenol-phenolate anion, hydrogen bond strength, $D(\text{PhO}^- \cdots \text{HOPh})$, can be determined by inputting the calculated and/or experimental values presented above into the following energetic relationship:

$$D(\text{PhO}^- \cdots \text{HOPh}) = \text{EA}((\text{PhO})_2\text{H}) + D(\text{PhO} \cdots \text{HOPh}) - \text{EA}(\text{PhO}) \quad (1)$$

Using only calculated values for the quantities on the right side of this equation yields a $D(\text{PhO}^- \cdots \text{HOPh})$ value of 1.21 eV (27.97 kcal/mol). This value is in excellent agreement with previous calculations performed at the composite CCSD(T) level with complete basis set (CBS) extrapolation (1.22 eV, 28.1 kcal/mol).¹⁰ Substituting only the experimentally very well-determined $\text{EA}(\text{PhO})$ value of 2.25 eV in Eqn. (1) implies a $D(\text{PhO}^- \cdots \text{HOPh})$ value of 1.12 eV (25.8 kcal/mol). Using the experimentally-determined values of both $\text{EA}(\text{PhO})$ and E_{T} , along with the computationally-derived value for $D(\text{PhO} \cdots \text{HOPh})$, implies a $D(\text{PhO}^- \cdots \text{HOPh})$ value of 1.27 eV (29.3 kcal/mol). All of these ways for finding $D(\text{PhO}^- \cdots \text{HOPh})$, i.e., the phenol-phenolate anion, ionic hydrogen bond strength, imply that it is quite strong. Pertinent values and relationships are exhibited in Table 1 and in Figure 2.

4. Discussion

Since hydrogen bonds are expected to be at their strongest in the gas phase, the estimated phenol-phenolate anion hydrogen bond strength (26-30 kcal/mol) we report here represents the maximum interaction strength of the PhO^-/HOPh couple in other environments. In the enzyme catalyzed reaction by ketosteroid isomerase (KSI), the dienolate intermediate is thought by some to be stabilized by a strong, low-barrier hydrogen bond (LBHB) involving a tyrosine hydroxyl (Tyr14) side chain. The PhO^-/HOPh hydrogen bond, i.e., $\text{PhO}^- \cdots \text{H}^+ \cdots \text{OPh}^-$, is a model for this interaction, and the interaction strength seen in this work suggests that it is a low barrier hydrogen bond.

The phenol/phenolate anion's hydrogen bond strength is ~60% of the hydrogen bond strength of HF_2^- (2.0 eV), the strongest known hydrogen bond.²⁶ This may seem surprising, since phenol is a very weak acid with a $\sim\text{pK}_{\text{a}}$ value of 10 (in water). What is responsible for its unexpected proton donating ability, and how can phenol form such strong hydrogen bonds? The

answer lies in the increased ring π -resonance of the hydrogen-bonded phenol. In the $\text{PhO}^- \cdots \text{HOPh}$ complex, hydrogen bonds can polarize the π -electrons in the phenol ring, enhance its “phenolate-like” character (see Figure 3, resonance structures on the right), and lead to increased π -electron delocalization. Note that increased π -conjugation does not necessarily reflect enhanced π -aromatic character. Upon hydrogen bonding, phenol exhibits increased net π -electron delocalization energy but reduced π -aromaticity, since the π -electrons are polarized towards the exocyclic C–O moiety (this reduces “cyclic” six π -electron character in the ring, see also resonance forms of the hydrogen bonded phenol in Figure 3, right). The degree of π -resonance (RE) increase can be estimated directly through BLW computations (see Methods). Based on this procedure (see Figure 3, left), the three π -bonds in phenol can be localized into three “blocks” (each corresponding to a localized π -molecular orbital with two π electrons); this disables π -conjugation, and when compared to the energy of the fully π -electron delocalized wavefunction, provides a measure of the RE of phenol. Remarkably, the computed BLW-RE for the hydrogen-bonded phenol (BLW-RE: 117.5 kcal/mol, in $\text{PhO}^- \cdots \text{HOPh}$) is +9.6 kcal/mol greater than that of the free phenol monomer (BLW-RE: 107.9 kcal/mol). This “extra” stabilization is significant and may contribute to the stronger than expected $\text{PhO}^- \cdots \text{HOPh}$ hydrogen bond strength.

The strength of the phenol-phenolate hydrogen bond is close to the previously measured gas-phase, intermolecular hydrogen bond strength of the proton-coupled pair imidazole-imidazolidine (0.9 eV).²⁶ Imidazole is also a very weak acid with a $\sim\text{pK}_a$ value of 14 (in water). The hydrogen bond strength in the imidazole–imidazolidine anionic complex, $\text{Im}^- \cdots \text{HIm}$, was estimated from the difference between the $E_T[\text{H}(\text{Im})_2]$ and $\text{EA}(\text{Im})$. Given that the hydrogen bonding interaction, $D(\text{PhO}^- \cdots \text{HOPh})$, in the neutral radical, $\text{Ph} \cdots \text{HPh}$, was not negligible in the estimation of the PhO^-/HOPh hydrogen bond strength, we calculated the hydrogen bonding interaction of neutral $\text{Im}^- \cdots \text{HIm}$ and found it to be 0.29 eV. Thus, our previously reported value of 0.9 eV may be a lower limit to the hydrogen bond strength of the Im^-/HIm complex. A previous gas phase measurement of the dissociation energy of HIm_2^- reported a value of 1.1 eV.²⁹ Thus, a hydrogen bond strength that is slightly greater than 0.9 eV for the imidazole–imidazolidine anionic complex would be reasonable and in good agreement with that measurement. In any case, the result of both the present work on PhO^-/HOPh and the previous work on Im^-/HIm is that the ionic hydrogen bond strengths of these enzymatically relevant models are very strong in the gas phase. If even a fraction of these hydrogen bond strengths were to be retained in enzyme active site environments, they might be able to facilitate enzymatic rate enhancements.

5. Conclusions

The hydrogen bonding in the phenol-phenolate anionic complex was studied experimentally using anion photoelectron spectroscopy and theoretically using density functional theory computations at the $\omega\text{B97XD}/6\text{-311+G}(2\text{d,p})$ level. The computed and experimentally-derived phenol-phenolate anion hydrogen bond strengths agree and are rather considerable. The unexpectedly strong bonding in the $\text{PhO}^- \cdots \text{HOPh}$ complex may be due to increased π -electron delocalization stabilization in the phenol ring.

Acknowledgements

This material is based on work supported by the National Science Foundation under Grant Numbers, CHE-1360692 (KHB) and CHE-1057466 (JIW).

References

1. R. F. Gunion, M. K. Gilles, M. L. Polak and W. C. Lineberger, *Int. J. Mass. Spectrom. Ion Processes*, 1992, **117**, 601.
2. A. R. McKay, M. E. Sanz, C. R. S. Mooney, R. S. Minns, E. M. Gill and H. H. Fielding, *Rev. Sci. Instrum.*, 2010, **81**, 123101.
3. J. B. Kim, T. I. Yacovitch, C. Hock and D. M. Neumark, *Phys. Chem. Chem. Phys.*, 2011, **13**, 17378.
4. H.-T. Liu, C.-G. Ning, D.-L. Huang, P. D. Dau and L.-S. Wang, *Angew. Chem. Int. Ed.*, 2013, **52**, 8976.
5. J. D. Steill, A. L. May, S. R. Campagna, J. Oomens and R. N. Compton, *J. Phys. Chem. A*, 2014, **118**, 8597.
6. T. B. McMahon and P. Kebarle, *J. Am. Chem. Soc.*, **1977**, 99, 2222.
7. J. E. Bartmess, J. A. Scott, R. T. McIver, Jr. *J. Am. Chem. Soc.*, 1979, **110**, 6046.
8. D. F. McMillen and D. M. Golden, *Ann. Rev. Phys. Chem.*, 1982, **33**, 493.
9. R. M. Borges dos Santos and J. A. M. Simoes, *J. Phys. Chem. Ref. Data*, 1998, **27**, 707.
10. M. Kolaski, A. Kumar, N. J. Singh and K. W. Kim, *Phys. Chem. Chem. Phys.*, 2011, **13**, 991.
11. T. M. Krygowski and H. Szatyłowicz, *J. Phys. Chem. A*, 2006, **110**, 7232.
12. A. K. Chandra and T. Uchamaru, *Int. J. Mol. Sci.*, 2002, **3**, 407.
13. A. Surjoosingh, S. Hammes-Schiffer, *J. Phys. Chem. A*, 2011, **115**, 2367-2377.
14. P. J. Lodi and J. R. Knowles, *Biochemistry*, 1991, **30**, 6948.
15. J. A. Gerlt and P. G. Gassman, *J. Am. Chem. Soc.*, 1993, **115**, 11552.
16. W. W. Cleland and M. M. Kreevoy, *Science*, 1994, **264**, 1887.
17. P. A. Frey, S. A. Whitt and J. B. Tobin, *Science*, 1994 **264**, 1927.
18. W. Childs and S. G. Boxer, *Biochemistry*, 2010, **49**, 2723.

19. Q. Zhao, C. Abeygunawardana, P. Talalay, and A. S. Mildvan, *Proc. Natl. Acad. Sci.*, 1996, **93**, 8220.
20. O. C. Thomas, W. J. Zheng, and K. H. Bowen, *J. Chem. Phys.*, 2001, **114**, 5514.
21. J.-D. Chai and M. Head-Gordon, *Phys. Chem. Chem. Phys.* 2008, **10**, 6615.
22. R. Krishnan, J.S. Binkley, R. Seeger and J.A. Pople, *J. Chem. Phys.* 1980, **72**, 650.
23. S. Simon, M. Duran, and J. J. Dannenberg, *J. Chem. Phys.*, 1996, **105**, 11024.
24. Gaussian 09, Revision **D.01**, M. J. Frisch, G. W. Trucks, H. B. Schlegel, G. E. Scuseria, M. A. Robb, J. R. Cheeseman, G. Scalmani, V. Barone, B. Mennucci, G. A. Petersson, H. Nakatsuji, M. Caricato, X. Li, H. P. Hratchian, A. F. Izmaylov, J. Bloino, G. Zheng, J. L. Sonnenberg, M. Hada, M. Ehara, K. Toyota, R. Fukuda, J. Hasegawa, M. Ishida, T. Nakajima, Y. Honda, O. Kitao, H. Nakai, T. Vreven, J. A. Montgomery, Jr., J. E. Peralta, F. Ogliaro, M. Bearpark, J. J. Heyd, E. Brothers, K. N. Kudin, V. N. Staroverov, R. Kobayashi, J. Normand, K. Raghavachari, A. Rendell, J. C. Burant, S. S. Iyengar, J. Tomasi, M. Cossi, N. Rega, J. M. Millam, M. Klene, J. E. Knox, J. B. Cross, V. Bakken, C. Adamo, J. Jaramillo, R. Gomperts, R. E. Stratmann, O. Yazyev, A. J. Austin, R. Cammi, C. Pomelli, J. W. Ochterski, R. L. Martin, K. Morokuma, V. G. Zakrzewski, G. A. Voth, P. Salvador, J. J. Dannenberg, S. Dapprich, A. D. Daniels, Ö. Farkas, J. B. Foresman, J. V. Ortiz, J. Cioslowski, and D. J. Fox, Gaussian, Inc., Wallingford CT, 2009.
25. Y. Mo, L. C. Song and Y. C. Lin, *J. Phys. Chem. A*, 2007, **111**, 8291.
26. J. D. Graham, A. M. Buytendyk, D. Wang, K. H. Bowen and K. D. Collins, *Biochemistry*, 2014, **53**, 344.
27. R. B. Metz, A. Weaver, S. E. Bradforth, T. N. Kitsopoulos, and D. M. Neumark, *J. Phys. Chem.*, 1990, **94**, 1377.
28. S. E. Bradforth, A. Weaver, D. W. Arnold, R. B. Metz, D. M. Neumark, *J. Chem. Phys.*, 1990, **92**, 7205.
29. Meot-Ner (Mautner), M. *J. Am. Chem. Soc.*, 1988, **110**, 3075.

Table 1: Computed EA(PhO), EA((PhO)₂H), and D(PhO...HOPh) values^a at ω B97XD/6-311+G(2*d*,*p*) [all values include zero-point vibrational energy (ZPVE) and basis set superposition error (BSSE) corrections]. The implied D(PhO⁻...HOPh) value provides a direct estimate of the PhO⁻...HOPh hydrogen bonding strength. Experimental values are listed in parenthesis for comparison.

EA(PhO)	EA ((PhO) ₂ H)	D(PhO...HOPh)	D(PhO ⁻ ...HOPh)
2.16	3.01	0.36	1.21
(2.25) ^b	(<i>E_T</i> = 3.16)	--	--

^a All values are presented in units of electron volts (eV).

^b Value taken from ref 4.

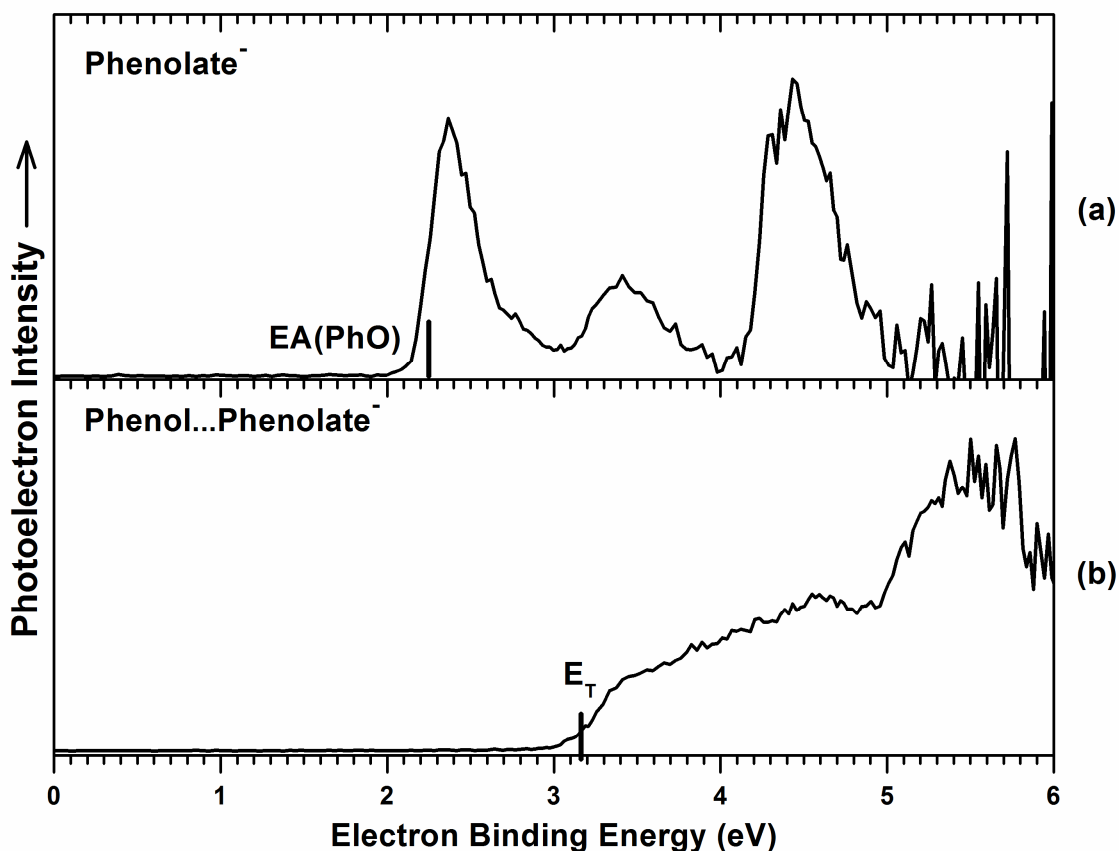


Figure 1: Anion photoelectron spectra of (a) the phenolate anion and (b) the phenol-phenolate anionic complex. All spectra were calibrated against the photoelectron spectrum of Cu⁻, the copper atomic anion.

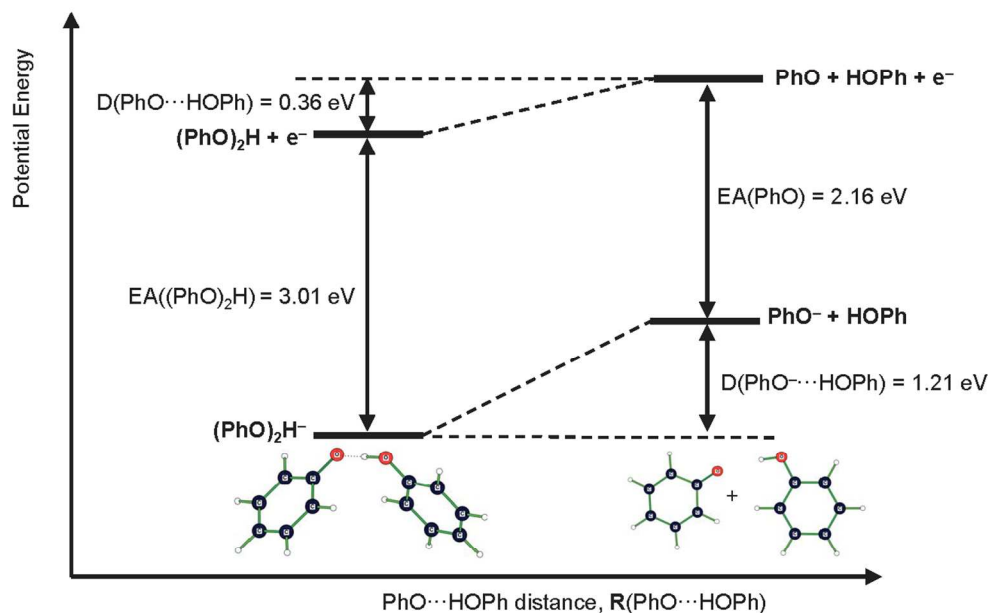


Figure 2: Schematic illustration of the energetic relationships between $EA(\text{PhO})$, $EA((\text{PhO})_2\text{H})$, $D(\text{PhO}\cdots\text{HOPh})$, and $D(\text{PhO}^-\cdots\text{HOPh})$ [all values include zero-point vibrational energy (ZPVE) and basis set superposition error (BSSE) corrections].

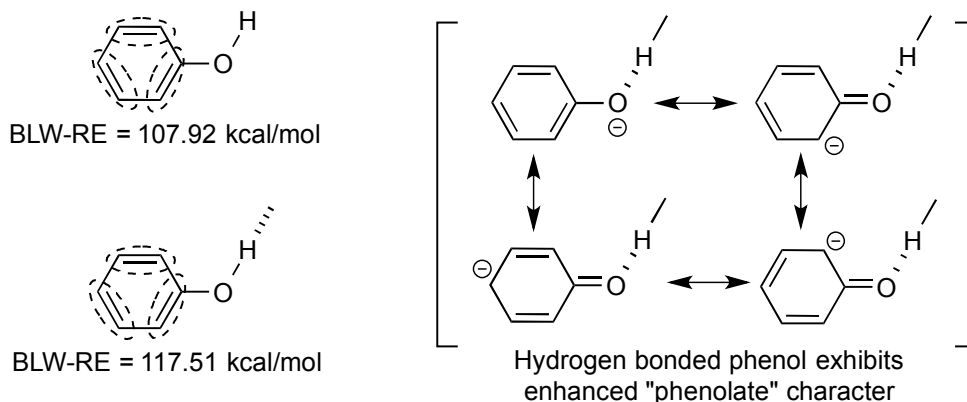


Figure 3: (On the left) Computed vertical BLW-RE's (in kcal/mol, at B3LYP/6-31G*) for the phenol monomer and hydrogen bonded phenol (in $\text{PhO}^-\cdots\text{HOPh}$). The dotted circles represent the three π -electron localized "blocks"; this BLW procedure disables π -conjugation in the ring and evaluates the π -RE's of phenol rings considered (see Methods). (On the right) Resonance structures of hydrogen bonded phenol rings all display enhanced "phenolate" character.